Identifying Fingerprint Alteration Using the Reliability Map of the Orientation Field

Adina Petrovici, Corneliu Lazar

Automatic Control and Applied Informatics Department, Technical University "Gheorghe Asachi", Iasi, Romania (e-mail:{apetrovici; clazar}@ac.tuiasi.ro)

Abstract: Fingerprint recognition is one of the most commonly used biometric technology. Even if fingerprint temporarily changes (cuts, bruises) it reappears after the finger heals. Criminals started to be aware of this and try to escape the identification systems applying methods from ingenious to very cruel. It is possible to remove, alter or even fake fingerprints (made of glue, latex, silicone), by burning the fingertip skin (fire, acid, other corrosive material), by using plastic surgery (changing the skin completely, causing change in pattern – portions of skin are removed from a finger and grafted back in different positions, like rotation or "Z" cuts, transplantations of an area from other parts of the body like other fingers, palms, toes, soles). This paper presents a new algorithm for altered fingerprints detection based on fingerprint orientation field reliability. The map of the orientation field reliability has peaks in the singular point locations. These peaks are used to analyze altered fingerprints because, due to alteration, more peaks as singular points appear with lower amplitudes.

Keywords: Fingerprints, alteration, image enhancement, reliability, singular points.

1. INTRODUCTION

Biometric recognition (or simply biometrics) refers to the use of distinctive anatomical (e.g., fingerprints, face, iris) and behavioral (e.g., speech) characteristics, called biometric identifiers or traits or characteristics for automatically recognizing individuals.

Every human being possesses fingers (with the exception of hand-related disability) and hence fingerprints. Fingerprints are very distinctive and they are permanent; even if they temporarily change slightly due to cuts and bruises on the skin, the fingerprint reappears after the finger heals.

Offenders have been focusing on circumventing and compromising biometric systems. Fake physical biometric represents a point of vulnerability because it is possible to reproduce artificially fake fingers in order to adopt somebody's else identity or to change ridge patterns by mutilating fingerprints, in order to mask his own identity.

Unnatural fingerprints used as fake biometric may be categorized into two types: *fake* or *altered*. Fake fingerprint represents a replica of a real fingerprint (from a live finger or a latent print) made up of artificial materials like gelatine, silicone, latex. The biometric device must decide if the finger on the acquisition sensor is "alive" or "fake". This procedure is called vitality detection (or liveness or spoof detection). Altered fingerprints are real fingerprints with changes made on the finger ridge pattern. Three types of degradations of the ridge patterns may be distinguished: *obliteration*, *distortion* and *imitation*. Obliterated fingerprints refer to the fingerprints resulting from abrading, cutting, burning, applying strong chemicals or transplanting smooth skin. The skin regenerates after a few months. Friction ridge patterns can be turned into distorted ridge patterns by plastic surgery. Portions of the skin are removed from the finger and transplanted back on the same finger on different positions. Imitation of the fingerprint is also made by plastic surgery but this involves the transplantation of a large-area friction skin from other parts of the body such as other fingers, palms, soles, toes. The biometric device must decide if the finger on the acquisition sensor is "natural" or "altered" and if the finger is altered must decide whose identity is trying to mask, by matching the altered fingerprint with the natural fingerprint (which is very likely to be stored in the database).

Unlike the problem of fingerprint alteration, the use of fake fingerprints has received increased attention in the literature. Methods of life detection have been proposed based on physiologic characteristics (pulse, temperature, odor, dielectric resistance) or behavioral characteristics (deformation of the skin, diffusion of sweat).

In scientific literature, hardware-base and software-based methods have been proposed to detect the fingerprint vitality. Software solutions refer to extracting features from the fingerprint image by comparing multiple frames called dynamic methods, perspiration based (Derakhshani *et al.*, 2003), (Parthasaradhi *et al.*, 2005), (Coli *et al.*, 2006) and elastic deformation based (Antonelli *et al.*, 2006). Static methods use single impression and are perspiration based (Tan and Schuckers, 2006) or morphology based (Moon *et al.*, 2005), or multiple impressions, elastic deformation based (Chen *et al.*, 2005) or morphology based.

The problem of identifying altered fingerprints was introduced by (Feng *et al.*, 2009). This paper is based upon obliteration of finger ridge patterns highlighting the reasons why offenders go to an extent of performing such act. A study regarding finger prints obfuscation problems is presented. In the same paper, an automatic detection

algorithm of altered fingerprints is given. The algorithm is based on detecting the singular points using Poincaré index from the orientation field of a fingerprint. Then, the singular points are removed in order to obtain a continuous orientation field from which a feature vector is extracted called histogram curvature and used as an input to a support vector classifier for distinguishing between natural and altered fingerprints. An analysis based on orientation field reliability was presented in (Petrovici and Lazar, 2010).

This paper presents a new method for altered finger prints detection based also on the orientation field of fingerprints. Using an orientation field, singular points are detected following an approach from (Khalil *et al.*, 2010) that uses fingerprint orientation field reliability. The orientation field reliability map has peaks in the singular point locations. These peaks are used to analyze altered fingerprints because due to alteration, more peaks as singular points appear with lower amplitudes. The experimental results on images from FVC2004, DB1, and a real altered fingerprint show that locating the position of singular point may be useful in detecting altered fingerprints.

The paper is organised as follows. In Section 2 the fingerprint image pre-processing stage is presented. In Section 3 the ridge orientation estimation method is described. The proposed algorithm for identifying fingerprint alteration is presented in Section 4 and experimental results are presented in Section 5. The paper is finished with the conclusions in Section 6.

2. FINGERPRINT IMAGE PRE-PROCESSING

The aim of the image pre-processing stage is to increase both the accuracy and the interpretability of the digital data during the image processing stage. The pre-processing takes place prior to any principal component analysis. The main steps for pre-processing are enhancement, binarization, distance transform and segmentation.

First, a pre-processing stage of image enhancement is performed in order to improve the contrast between ridges and valleys and reduce noises in the fingerprint images. Two methods are adopted for image enhancement stage: the first one is based on Histogram Equalization and the next one on Fourier Transform. A local adaptive binarization method is performed to binarize the fingerprint image.

The binary image obtained after image enhancement is transformed into gray scale image using the euclidean distance transform.

Fingerprint segmentation is implemented, to decide which part of the image belongs to the foreground and which part belongs to the background. The singular points will be located more accurately if the localization operates only on the foreground of the fingerprint image.

2.1 Image Enhancement

The fingerprint input image is enhanced in the spatial domain by applying the Histogram Equalization technique, for a better distribution of the pixel values. Considering the real altered fingerprint from Fig. 1(a), the result image is represented in Fig. 1(b).

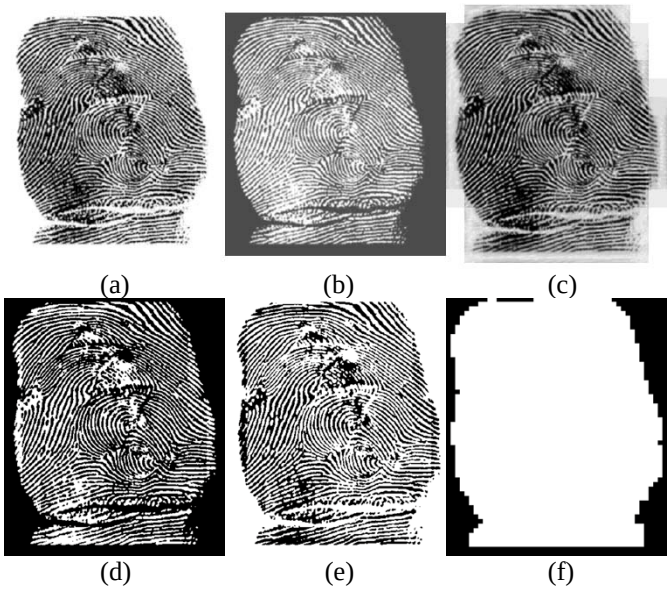

Fig. 1 Pre-processing steps: a). Real altered fingerprint image; b). Image obtain after Histogram Equalization; c). Image obtained after FFT; d). Binary image; e). Distance transform image; f). Region of interest.

The histogram of a digital image with gray levels in the range [0, *L*-1] is a discrete function:

$$P(r_k) = \frac{n_k}{n}, \qquad (1)$$

where r_k represents the k'th gray level, n_k is the number of pixels in the image with that gray level, n represents the total number of pixels in the image, $k = 0,1,...,L, L = 256$.

In the frequency domain, the fingerprint image is enhanced based on the Fast Fourier Transform (FFT), Fig. 2(c).

The image is divided into $32x32$ processing blocks and the Fourier Transform is performed according to:

$$F(u,v) = \sum_{i=0}^{M-1}\sum_{j=0}^{N-1} f(i,j)x\exp\{-j2\pi(\frac{ui}{M}+\frac{vj}{N})\}, \qquad (2)$$

for $u = 0,1,...,31, v = 0,1,...,31$.

In order to enhance a specific block by its dominant frequencies, the FFT of the block is multiplied by its magnitude a set of times, where the magnitude of the original FFT is:

$$FFT = abs(F(u,v)) = |F(u,v)|. \qquad (3)$$

The enhanced block is obtained according to:

$$g(i,j) = F^{-1}\{F(u,v)x|F(u,v)|^k\}, \qquad (4)$$

where $F^{-1}(F(u,v))$ is computed using:

$$f(i,j) = \frac{1}{MN}\sum_{i=0}^{M-1}\sum_{j=0}^{N-1} F(u,v)x\exp\{\, j2\pi(\frac{ui}{M}+\frac{vj}{N})\}, \quad (5)$$

for $u = 0,1,...,31, v = 0,1,...,31$. The experimentally constant k is set to 0.45 (a higher k improves the appearence of the ridges, filling up small holes in ridges; a very high k may introduce false joining of ridges).

2.2 Distance Transform and Image Segmentation

The distance transform of the binary image, Fig. 1(d), is defined as the distance from every black pixel (belonging to the fingerprint ridges) to the nearest white pixel. The euclidean distance between two pixels (i_1, j_1) and (i_2, j_2) is defined as:

$$d_{euclid}((i_1,j_1),(i_2,j_2)) = \sqrt{(i_1-i_2)^2+(j_1-j_2)^2}\ . \quad (6)$$

In order to mark the foreground and background images, a blockwise ($8x8$ pixels) binary image is created based on the distance transform image, represented in Fig. 1(e). A block of $8x8$ pixels is set as foreground if at least 80% of its pixels have values smaller than a threshold (set to 10.), Fig. 1(f). For each block in the foreground, the orientation field is estimated applying a gradient-based method, based on the distance transform image.

3. RIDGE ORIENTATION ESTIMATION

The orientation field image is a Level 1 feature that represents the angle $\theta_{i,j}$, shown in Fig. 2, that the finger print ridges form with the horizontal axis, crossing through an arbitrary small neighbourhood centered at (i, j).

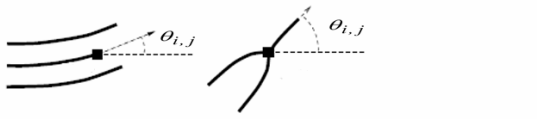

Fig. 2 Ridge ending and ridge bifurcation orientation angle

This is a gradient based method (Hong *et al.*,1998). A single orientation is assigned for each non-overlapping block of size wxw ($16x16$ pixels) that corresponds to the dominant orientation of the block.

The gradient G at the point (i, j) is computed as a 2 dimensional vector with the components $G_x(i, j)$ and $G_y(i, j)$ the horizontal and the vertical gradients, with respect to the *x* and *y* directions. Simple gradient operators are used such as a Sobel mask ($3x3$).

The local orientation of each block centered at pixel (i, j) is estimated using the following equations:

$$V_x(i,j) = \sum_{u=i-\frac{W}{2}}^{i+\frac{W}{2}}\sum_{v=j-\frac{W}{2}}^{j+\frac{W}{2}} 2G_x(u,v)G_y(u,v),$$

$$V_y(i,j) = \sum_{u=i-\frac{W}{2}}^{i+\frac{W}{2}}\sum_{v=j-\frac{W}{2}}^{j+\frac{W}{2}} (G_x^2(u,v)-G_y^2(u,v)), \quad (7)$$

$$\theta(i,j) = \frac{1}{2}tan^{-1}(\frac{V_y(i,j)}{V_x(i,j)}),$$

where $\theta(i, j)$ is the least square estimate of the local ridge orientation at the block centered at pixel (i, j).

In order to adjust the incorrect local ridge orientation, due to the presence of noise, a low-pass filtering can be used, since local ridge orientation varies slowly in a local neighbourhood where singular points appear. The orientation image needs to be converted into a *continuous vector field*, as follows:

$$\Phi_x(i,j) = cos(2\theta(i,j)),$$
$$\Phi_x(i,j) = cos(2\theta(i,j)), \quad (8)$$

where $\Phi_x(i, j)$ and $\Phi_y(i, j)$ are components of the vector field. With the resulting vector field, the low-pass filtering can be performed as follows:

$$\Phi'_x(i,j) = \sum_{u=-\frac{w_\Phi}{2}}^{\frac{w_\Phi}{2}}\sum_{v=-\frac{w_\Phi}{2}}^{\frac{w_\Phi}{2}} W(u,v)\Phi_x(i-uw, j-vw),$$
$$\Phi'_y(i,j) = \sum_{u=-\frac{w_\Phi}{2}}^{\frac{w_\Phi}{2}}\sum_{v=-\frac{w_\Phi}{2}}^{\frac{w_\Phi}{2}} W(u,v)\Phi_y(i-uw, j-vw), \quad (9)$$

where W is a 2-dimensional low-pass filter with unit integral and $w_\Phi x w_\Phi$ specifies the size of the filter (default size $5x5$).

After the smoothing operation is performed at the block level, the local ridge orientation at (i, j) is computed using:

$$O(i,j) = \frac{1}{2}tan^{-1}(\frac{\Phi'_y(i,j)}{\Phi'_x(i,j)}), \quad (10)$$

where $O(i, j)$ represents the orientation image.

4. ALGORITHM FOR IDENTIFYING FINGERPRINT ALTERATION

The algorithm is implemented based on analyzing the ridge orientation field, in order to compute the orientation field reliability (Khalil *et al.*, 2010). The reliability of the orientation field describes the consistency of the local orientations in a neighbourhood along the dominant orientation; it is used to locate the unique singular point constantly for all types of fingerprints.

Based on the distance transform image, the method presented in Section 3 is implemented to obtain the orientation field and the orientation field reliability. The least mean square method of orientation based on the gradients is most widely used to compute the dominant orientation of an image block because of its high efficiency and resolution. Since the gradient phase angle is the orientation with maximum grey value change, it is orthogonal to the local ridge orientation of each pixel.

The continuous vector field is obtained in order to perform the low-pass filtering. The Gaussian filter is applied, having the size of $w_\Phi x w_\Phi$ set to $5x5$. The local ridge orientation is obtained.

The method measures the strength of the peaks computing first:

$$\begin{aligned} min\_inertia(i,j) &= (G_{yy}(i,j)+G_{xx}(i,j)) \\ &-(\Phi'_x(i,j)G_{xx}(i,j)-G_{yy}(i,j)) \\ &-(\Phi'_y(i,j)G_{xy}(i,j))/2, \\ max\_inertia(i,j) &= G_{yy}(i,j)+G_{xx}(i,j) \\ &- min\_inertia(i,j), \end{aligned} \tag{11}$$

where:

$$\begin{aligned} G_{xx}(i,j) &= \sum_{u=i-\frac{w}{2}}^{i+\frac{w}{2}} \sum_{v=j-\frac{w}{2}}^{j+\frac{w}{2}} G_x(u,v)G_x(u,v), \\ G_{yy}(i,j) &= \sum_{u=i-\frac{w}{2}}^{i+\frac{w}{2}} \sum_{v=j-\frac{w}{2}}^{j+\frac{w}{2}} G_y(u,v)G_y(u,v), \\ G_{xy}(i,j) &= \sum_{u=i-\frac{w}{2}}^{i+\frac{w}{2}} \sum_{v=j-\frac{w}{2}}^{j+\frac{w}{2}} G_x(u,v)G_y(u,v). \end{aligned} \tag{12}$$

Having *min_inertia* and *max_inertia* from (11), the reliability R is given by:

$$R(i,j) = 1 - \frac{min\_inertia(i,j)}{max\_inertia(i,j)}. \tag{13}$$

Based on the method described for field orientation estimation and the computation of the reliability R, the following algorithm is proposed, for altered fingerprint detection:

Stage 1: Pre-processing

Equalize histogram

For each block of size $32x32$ apply Fast Fourier Transform

For each block of size $32x32$ binarize enhanced image ($threshold = 0.8xmean(block\_intensity)$).

Apply distance transform image

For each block of size $8x8$ pixels belonging to the distance transform image, segmentate image

Stage 2: Orientation field before filtering and continuous vector field

For each pixel (i,j) in the distance transform image compute the horizontal and vertical gradients $G_x(i,j)$ and $G_y(i,j)$, using Sobel mask ($3x3$)

For each block of size wxe ($16x16$) centered at pixel (i,j)

If the block belongs to the foreground

Compute $V_x(i,j)$, $V_y(i,j)$

Compute $G_{xx}(i,j)$, $G_{yy}(i,j)$, $G_{xy}(i,j)$

Compute $\theta(i,j) = a\tan 2(V_y(i,j),V_x(i,j))/2$

Compute components of the continuous vector field $\Phi_x(i,j)$ and $\Phi_y(i,j)$

End if

End for

Stage 3: Orientation field and reliability orientation image

For each block of size wxw ($16x16$) centered at pixel (i,j).

If the block belongs to the foreground

Compute

$\Phi'_x(i,j) = sum(sum(W(u,v)\Phi_x(i-uw,j-vw)))$

Compute

$\Phi'_y(i,j) = sum(sum(W(u,v)\Phi_y(i-uw,j-vw)))$

Compute $O(i,j) = a\tan 2(\Phi'_y(i,j),\Phi'_x(i,j))/2$

Compute $min\_inertia(i,j)$ and $max\_inertia(i,j)$

Compute $R(i,j)$

End if

End for

The algorithm for altered fingerprint detection has been implemented in MATLAB.

By observing the plot in the three-dimensional space of the reliability R obtained from the proposed method, we can identify high peak amplitudes that can be used to detect natural fingerprints and more smaller peak amplitude that can be used to detect altered fingerprints

5. EXPERIMENTAL RESULTS

The natural fingerprints are compared with the altered fingerprints, by observing the values of the reliability singular points. In this paper, the singular point is defined as the point with maximum curvature on the convex ridge. For natural fingerprints, the reliability orientation image generally has one sharp peak, while in altered fingerprints more peaks are

detected with smaller values. Starting from this observation, the altered fingerprint analysis can be done using the density and the amplitude of the peaks of the singular points.

The proposed algorithm for fingerprint analysis based on the estimation of orientation field and the computation of the reliability was tested with real altered fingerprint and simulated altered fingerprint obtained from natural fingerprint images from FVC2004, DB1, captured with optical sensor, with size 640x480, at a resolution of 500dpi.

The real altered fingerprint by distortion, "Z" cut shaped is shown in Fig 3 (a). Experimental results show that multiple peaks are detected as singular points, with lower amplitude, represented in Fig. 3 (d). The maximum positive amplitude has a value of 556 and the minimum negative amplitude has a value of -54.

In the absence of the natural (unaltered) fingerprint of the real altered fingerprint shown in Fig. 3(a) and due the lack of a database with altered fingerprint images, further analysis is necessary to be done on synthesized altered fingerprints. Two types of alterations are simulated:

(i) "Z" cut (obtained by making a "Z" shaped cut on the fingertip, lifting and switching the two triangles, and stitching them back);

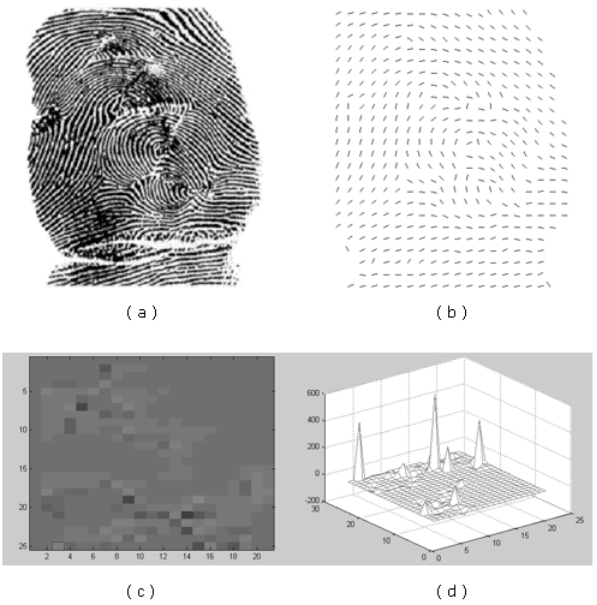

Fig. 3 (a) Real altered fingerprint, (b) Orientation field, (c) Orientation field reliability map and (d) Peaks indicating the singular points.

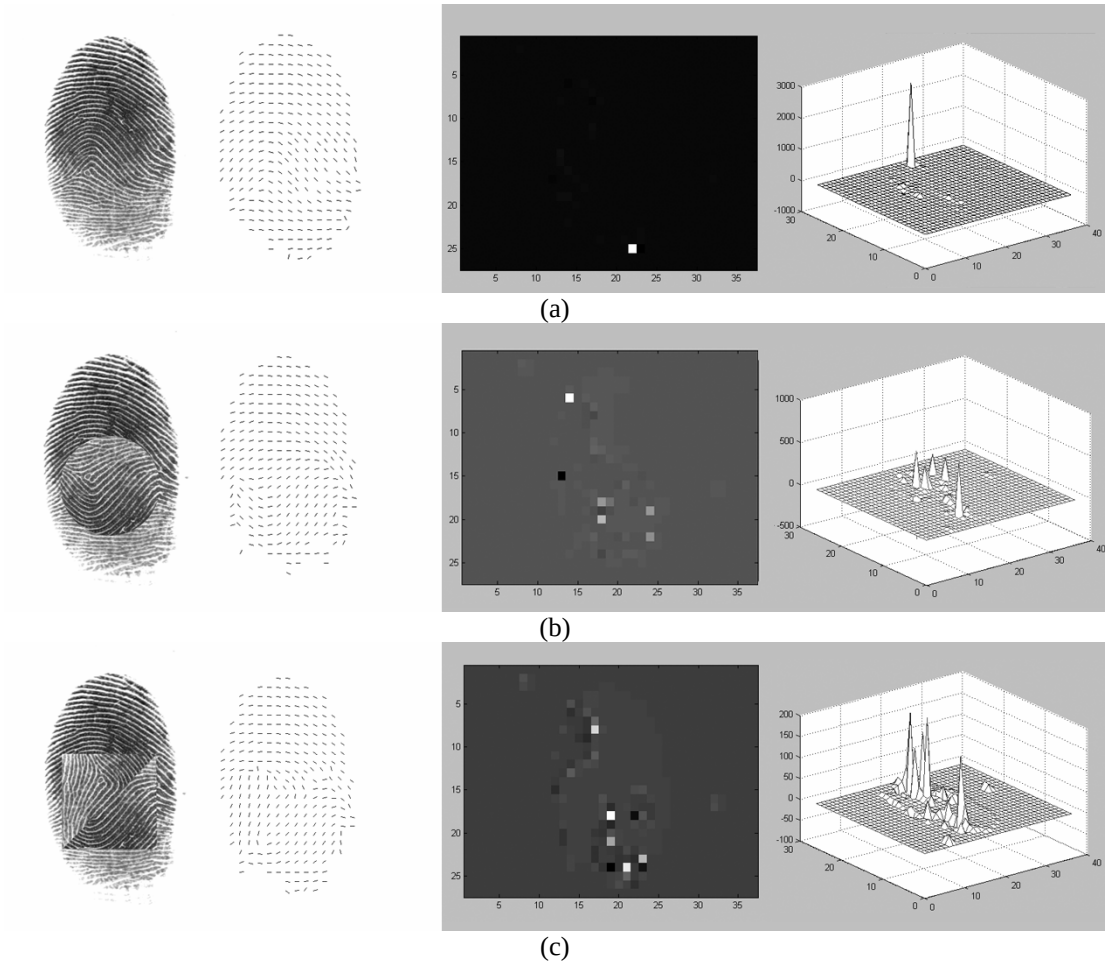

Fig. 4 Peaks detected in (a) a natural arch type fingerprint, (b) an altered fingerprint by central rotation and (c) an altered fingerprint by "Z" cut. From left to right: input image, orientation field, 2D reliability map, peaks indicating singular points.

(ii) central rotation (obtained by cutting a circular region and rotated by different degrees).

The arch type of a natural fingerprint and the corresponding altered forms obtained by central rotation and "Z" cut together with their orientation fields are considered in Fig. 4. The orientation field reliability map and the peak of the singular points for an arch type fingerprint are represented. The peak from the natural fingerprint in Fig 4(a) has a high value of 2644. The two altered fingerprint images, have more peaks, but with small values between 641 for the highest positive peak and -461 for the negative peak.

The next analysis was done considering the loop type natural fingerprint and its altered forms obtained by central rotation and "Z" cut from Fig. 5. In the same figure the orientation fields of the above fingerprints are given.

For the loop type natural fingerprint represented in Fig. 5(a), a negative peak with a high value of –1558 is found. For the image from Fig. 5(b), the peaks found have also small values between 249 and -836, like the results obtained with the arch type fingerprint images and with real altered fingerprint. The peaks from the image in Fig. 5(c) vary between 247 and -105.

The next fingerprint of type double loop and the orientation field are represented in Fig. 6(a) together with the two types of alterations (i), Fig. 6(b) and (ii), Fig. 6(c). The double loop type natural fingerprint has one peak with high negative value of -3175. The values of the peaks from the two altered fingerprints varies from 590 for the distortions introduced in Fig. 6(b) and -647 for the negative peak and 407 for the positive peak in Fig. 6(c), respectively.

The orientation field reliability maps represented in Fig. 4, Fig. 5 and Fig. 6 represent the localization of the singular points in the two-dimensional space. The gray level is determined by *R* and is proportional with the strength of the peaks.

The results obtained on the real altered fingerprint are corresponding with the results obtained from the simulated altered fingerprints.

In (Feng *et al.*, 2009), it was pointed out that using a feature vector termed as curvature histogram, extracted from the continuous vector field, as an input to train LIBSVM, an integrated software for support vector classification, leads to results showing that 92% altered fingerprints can be correctly detected.

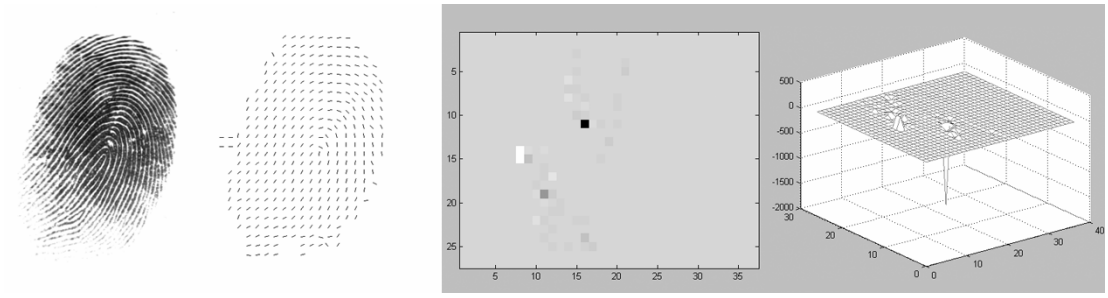

(a)

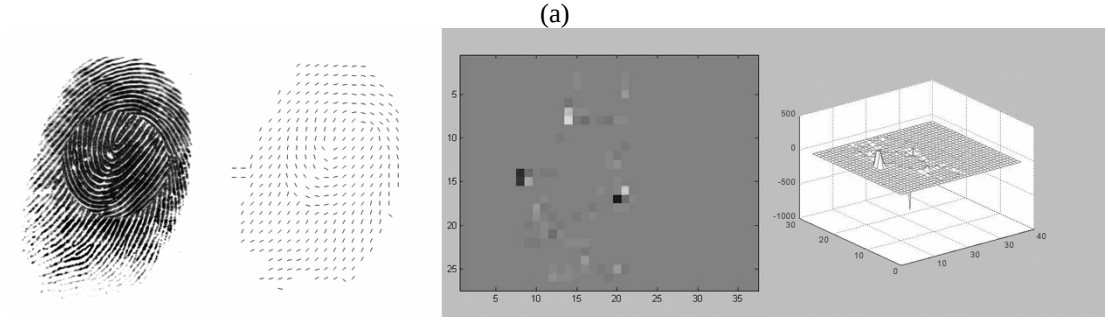

(b)

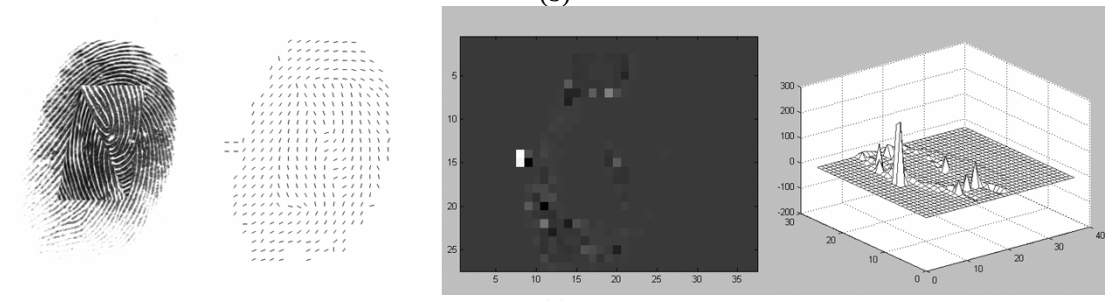

(c)

Fig. 5 Peaks detected in (a) a natural loop type fingerprint, (b) an altered fingerprint by central rotation and (c) an altered fingerprint by "Z" cut. From left to right: input image, orientation field, 2D reliability map, peaks indicating singular points.

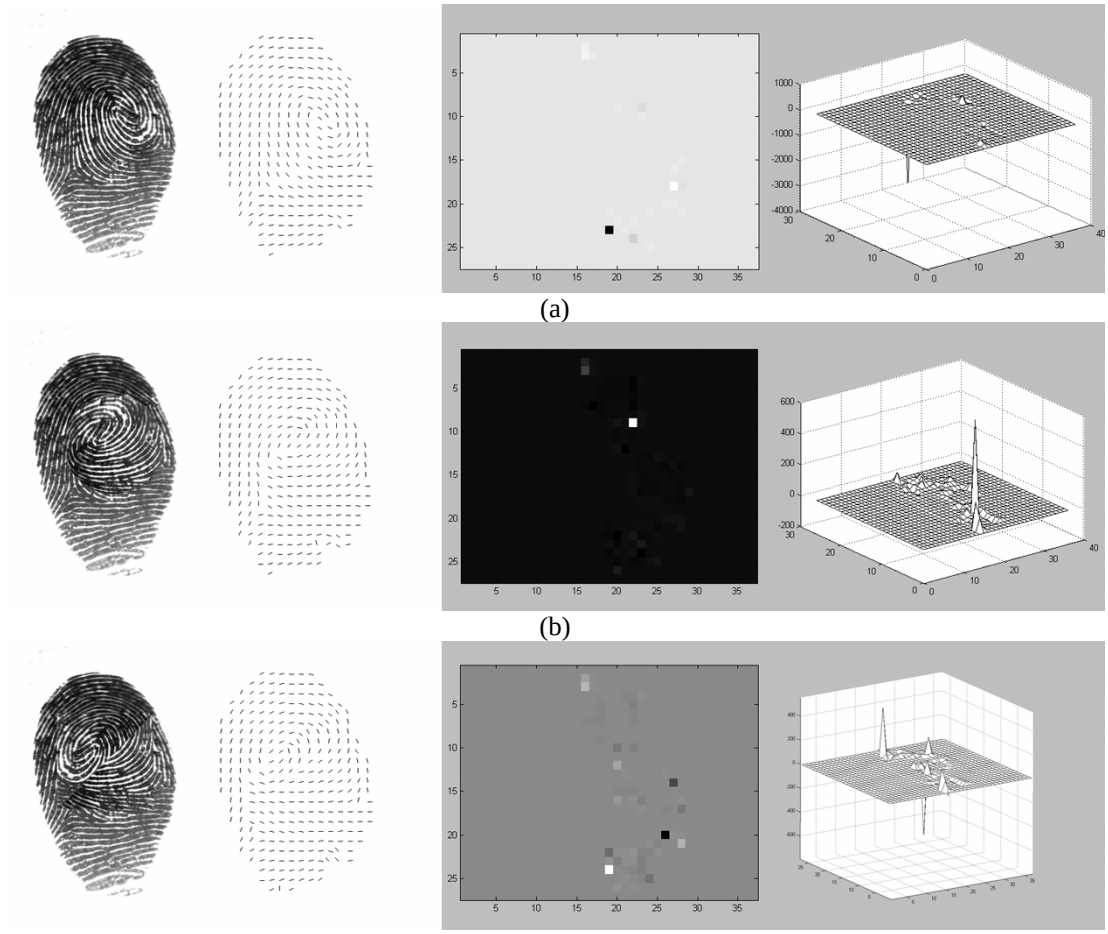

Fig. 6 Peaks detected in (a) a natural loop type fingerprint, (b) an altered fingerprint by central rotation and (c) an altered fingerprint by "Z" cut. From left to right: input image, orientation field, 2D reliability map, peaks indicating singular points.

In this work, singular points are detected with high amplitudes for natural fingerprints, and relatively small amplitudes for altered fingerprints, that can be used for classifying algorithms, in order to give a completely comparative study.

Testing the efficiency of the orientation field reliability, the experimental results indicate that the reliability *R* has strong information that can be used for future research. The singular value decomposition of *R* leads to obtaining essential features for discrimination and has good stability. The results obtained in altered fingerprints analysis using orientation field reliability are persuasive and could be employed for automatic detection of biometric obfuscation.

The proposed algorithm is tested on real altered fingerprint and synthetically altered images, in the absence of a real altered fingerprints and their matching natural fingerprints database.

6. CONCLUSIONS

This paper presented a method to analyze natural fingerprints and distorted fingerprints, based on the field orientation reliability. Using an orientation field, singular points are detected based on the fingerprint orientation field reliability. The orientation field reliability map has peaks in the singular point locations and these peaks are used to analyze altered fingerprints. Due to alteration, more peaks as singular points appear with lower amplitudes.

The experimental results demonstrate that the proposed algorithm can provide important information in order to automatically detect altered fingerprints.

REFERENCES

Antonelli, A., Cappelli, R., Maio, D., Maltoni, D., (2006), Fake Finger Detection by Skin Distortion Analysis, *IEEE Transactions on Information Forensics and Security*, volume 1 (no. 3), 360-373.

Chen, Y., Jain, A. K., Dass, S., (2005), Fingerprint Deformation for Spoof Detection, *Biometric Symposium*, Cristal City, VA.

Coli, P., Marcialis, G. L., Roli, F., (2006), Analysis and Selection of Feature for the Fingerprint Vitality Detection, *SSPR/SPR 2006*, 907-915.

Derakhshani, R., Schuckers, S., Homak, L., O'Gorman, L., (2003), Determination of Vitality from a Non-Invasive Biomedical Measurement for Use in Fingerprint Scanners, *Pattern Recognition* 36 (2), 383-396.

Feng, J., Jain, A. K., Ross, A., (2009), Fingerprint Alteration, *MSU Technical Report*, MSU-CSE-09-30.

Hong, L., Wan, Y., Jain, A. K., (1998), Fingerprint Image Enhancement: Algorithm and Performance Evaluation, *IEEE Transactions on Pattern Analysis and Machine Intelligence*, volume 20 (no. 8), 777-789.

Khalil, M. S., Muhammad, D., Khan, M. K., Alghathbar, K., (2010), Singular Points Detection using Fingerprint Orientation Field Reliability, *International Journal of Physical Sciences*, volume 5 (no. 4), 352-357.

Moon, Y. S., Chen, J. S., Chan, K. C., So, K., Woo, K. C., (2005), Wavelet Based Fingerprint Liveness Detection, *Electronics Letters*, volume 41 (no. 20), 1112-1113.

Parthasaradhi, S., Derakhshani, R., Homak, L., Schuckers, S., (2005), Time-series Detection of Perspiration as a Vitality Test in Fingerprint Devices, *IEEE Transactions on Systems, Man and Cybernetics*, part C, volume 35 (no. 3), 335-343.

Petrovici, A., Lazar, C., (2010), Altered Fingerprint Analysis Based on Orientation Field Reliability, accepted for *14th International Conference on System Theory and Control*, Romania, Sinaia.

Tan, B., Schuckers, S., (2006), Liveness Detection for Fongerprint Scanners Based on the Statistics of Wavelet Signal Processing, *Conference on Computer Vision Pattern Recognition Workshop*.